AIAA JOURNAL
Vol. 36, No. 6, June 1998

Interacting Vortex and Vortex Layer: How Length Scale Affects Entrainment and Ejection

Oliver V. Atassi,* Andrew J. Bernoff,† and Seth Lichter‡
Northwestern University, Evanston, Illinois 60208

A contour dynamics model of the interaction between a point vortex and a layer of constant vorticity, bounded below by a slip wall and above by irrotational flow, is studied. The height of the vortex above the layer establishes a length scale that is found to have a strong influence on both the evolution of the layer and the vertical displacement of the vortex. A vortex far above the boundary layer generates long-wavelength disturbances. These exhibit early-time growth, which saturates, taking on the shape of a vortex-like structure, suggesting that a vortex far above a boundary layer can create another one within the layer. Concurrently, entrainment of irrotational flow deep into the layer occurs within a narrow crevice. Alternatively, for a vortex initially placed close to the layer, a short-scale disturbance occurs that exhibits rapid, continuous growth that eventually rolls up around the vortex. Here, accounting for the vertical displacement of the vortex is necessary to accurately determine the interface evolution. The results support the contention that a vortex can induce ejection and roll up of the boundary layer and entrainment of irrotational flow into the layer.

I. Introduction

FOR certain shear flows, it has been found useful to assume that, although a viscous mechanism may be responsible for the initial distribution of vorticity, its subsequent evolution is dominated by inviscid interactions. Pullin[1] studied the evolution of disturbances on a wall-bounded layer of uniform vorticity underlying an inviscid flow. He found that large disturbances resulted in the ejection of thin filaments of vorticity into the irrotational flow (see also Ref. 2). Subsequent studies attempted to determine the mechanism by which the thin filaments interacted with the irrotational flow.[3,4] Jiménez and Orlandi[5] considered the inviscid roll up of a thin vortex layer. Geophysical interests have motivated studies on the interaction of a vortex with an infinite shear layer.[6–8]

This paper considers the two-dimensional inviscid interaction of a wall-bounded vortex layer with a point vortex. The utility of an inviscid approach may be justified as follows. Consider the inviscid timescale $T_\Gamma \equiv L^2/\Gamma$ due to the induced velocity of a point vortex of strengh Γ, where L is a length scale. Viscous diffusion occurs on a timescale $T_\nu \equiv L^2/\nu$. The ratio of the timescales defines a Reynolds number. For $T_\nu/T_\Gamma = \Gamma/\nu \to \infty$, viscosity has no opportunity to diffuse into the flow as it evolves on the faster inviscid timescale. Consequently, at high Reynolds numbers we expect the flow to evolve by an inviscid mechanism such as described here.

The contour dynamics model[9] we are presenting follows the formulation of Pullin.[1] The formulation permits multivalued deformations of the interface, which occur in overturning and roll-up phenomena. The model results yield not only the location of the interface but also the trajectory of the point vortex.

We focus on the effects of the length scale of the disturbance on the evolution of the boundary layer. The height of the vortex determines this length scale: Increasing (decreasing) the initial height of the vortex spreads its effect over a wider (narrower) interval on the interface. Initial conditions in which the length scale is varied are selected, whereas the variation of vortex-induced velocity is minimized. To this end, the ratio of the vortex circulation to the initial height of the vortex above the interface is fixed. As a result, for a vortex far above the wall, the initial velocity on the interface is the same at leading order for all cases when viewed as a function of the distance along the interface scaled with the vortex height (see Sec. IV).

Not only does the vortex act to deform the interface, but also the deformed interface induces a velocity on the point vortex. Consequently, the initial height of the vortex also sets the degree to which the boundary-layer deformations alter the path of the vortex. Namely, the velocity induced by the deformation on the vortex diminishes with distance. Whereas the vertical displacement of a distant vortex will be dynamically insignificant, in other cases the vortex will be strongly induced toward (away from) the interface, thus significantly enhancing (abating) its effect on the interface.

This work and those cited earlier are to be contrasted with viscous studies based on the boundary-layer equations.[10–15] The earliest of these studies ignored the changes induced in the outer flow as the boundary layer thickened. Recently, interacting boundary-layer formulations (IBL) have been incorporated to account for the effect of the boundary layer on the motion of the vortex. IBL methods have successfully described the early evolution of ejection. Furthermore, it has been shown that a new interactive singularity occurs in the IBL formulations that precedes the singularity found in the noninteracting boundary-layer models.[12] Consequently, a long-standing issue has been the extent to which modification of the vortex trajectory affects the evolution of the boundary layer.

The objectives of this work are 1) to investigate the role of the length scale of the disturbance and 2) to determine the conditions for which the displacement of the vortex significantly modifies the evolution of the boundary layer. In Sec. II we present the formulation of the model. Section III briefly describes the numerical method of solution and its validation. Section IV discusses our choice of scaling. Section V describes the numerical results. Finally, in Sec. VI we discuss the results, and in Sec. VII we draw conclusions from those numerical results.

II. Formulation

The two-dimensional, inviscid, incompressible flow is divided into two regions: an inner region D_+ of constant vorticity ω adjacent to the wall and an outer region D_- of irrotational flow extending to infinity with a freestream velocity U. The vortex layer extends upstream to $-\infty$ and downstream to $+\infty$ where it has constant thickness H_∞, and thus $\omega = U/H_\infty$. The two regions are separated by an interface located at $y = H(x, t)$ (Ref. 1).

A coordinate system (x, y) moving with the freestream velocity U and with the x axis parallel to the wall and the y axis perpendicular to it is now considered. In this frame of reference, the fluid velocity vanishes as $y \to \infty$, and the wall, located at $y = 0$, appears to be moving to the right. We nondimensionalize all lengths with respect

Presented as Paper 96-2140 at the AIAA 1st Theoretical Fluid Mechanics Meeting, New Orleans, LA, June 17–20, 1996; received April 19, 1997; revision received Jan. 21, 1998; accepted for publication Jan. 25, 1998.

*Research Assistant, Department of Mechanical Engineering.
†Assistant Professor, Department of Engineering Sciences and Applied Mathematics.
‡Professor, Department of Mechanical Engineering.

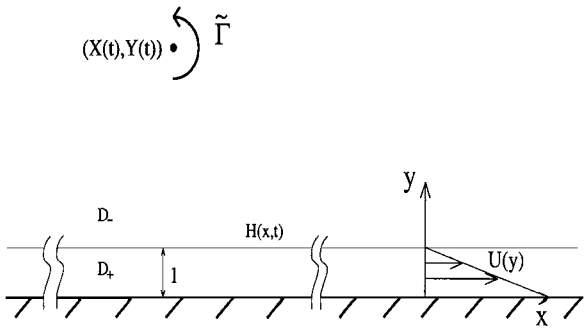

Fig. 1 Schematic of the geometry in dimensionless variables in a coordinate system moving with the uniform freestream velocity. In this coordinate system, the wall is moving to the right and the freestream velocity is zero. A vortex of circulation $\tilde{\Gamma}$ is located a distance $Y(t)$ above the wall. Here we show the initial conditions for a flat interface $H(x, 0) = 1$ and $Y(0) > 1$.

to H_∞ and time with respect to H_∞ / U. The geometry of the model is shown in Fig. 1. A vortex of circulation $\tilde{\Gamma}$ is located a distance $Y(t)$ above the wall.

The velocity field is the superposition of the velocities induced by the vortex layer and the vortex. Using a complex representation, the complex conjugate of the velocity is then

$$u - iv = \frac{1}{2\pi i}\iint_{D_+}\left(\frac{1}{z - z'} - \frac{1}{z - \bar{z}'}\right) dA' + \frac{\tilde{\Gamma}}{2\pi i}\left(\frac{1}{z - Z} - \frac{1}{z - \bar{Z}}\right) \tag{1}$$

where z' represents the source point and z the observation point. The location of the vortex in the complex plane is denoted $Z = X(t) + iY(t)$, and the nondimensional parameter $\tilde{\Gamma} = \Gamma/(\omega_\infty H_\infty^2)$ represents the ratio of the strength of the point vortex to the circulation in the layer. We apply the Stokes theorem[16] to transform the double integral over the area D_+ to a line integral over the contour C enclosing the region D_+. This yields

$$u - iv = \frac{1}{2\pi i}\left(\oint_C \frac{y' - y}{z' - z}\, dz' - \oint_C \frac{y' - y}{\bar{z}' - z}\, d\bar{z}'\right) + \frac{\tilde{\Gamma}}{2\pi i}\left(\frac{1}{z - Z} - \frac{1}{z - \bar{Z}}\right) \tag{2}$$

where the direction of integration is chosen to be counterclockwise. The terms that arise from integration over the vortex layer, region C, account for the deformation that the layer induces on itself; this self-interaction occurs only after the layer is perturbed. The terms proportional to the vortex strength $\tilde{\Gamma}$ are due to the vortex and its image in the wall.

The motion of the point vortex depends on its interaction with the boundary layer and the wall, and so its complex-conjugate velocity is given by

$$u_V - iv_V = \frac{1}{2\pi i}\left(\oint_C \frac{y' - Y}{z' - Z}\, dz' - \oint_C \frac{y' - Y}{\bar{z}' - Z}\, d\bar{z}'\right) + \frac{\tilde{\Gamma}}{4\pi Y} \tag{3}$$

where u_V and v_V are the horizontal and vertical velocities of the vortex. The first two terms on the right-hand side account for the motion of the vortex due to deformations of the boundary layer. The term proportional to the vortex strength $\tilde{\Gamma}$ accounts for the effect of the image vortex. Note that this term affects only the horizontal component of the vortex velocity v_V. The vertical displacement of the vortex away from its initial height is due to the deformation of the boundary layer, a relationship that is made precise in the next section.

We must also specify the initial shape of the interface, $y = H(x, 0) = H_0(x)$. Here, we consider only an initially flat interface, $H_0(x) = 1$. The final boundary condition is the kinematic condition that a fluid particle on the interface will remain on the interface:

$$v = \frac{\partial H}{\partial t} + u\frac{\partial H}{\partial x} \qquad \text{at} \qquad y = H(x, t) \tag{4}$$

Thus, the fully nonlinear interaction between a wall-bounded vortex layer and a point vortex is formulated in terms of an initial value problem involving three coupled equations, Eqs. (2–4).

III. Numerical Method and Validation

To numerically calculate the Lagrangian evolution of the interface and the pathline of the vortex, Eqs. (2) and (3) must be integrated spatially, followed by the temporal integration of

$$\frac{dx}{dt} = u \tag{5}$$

$$\frac{dy}{dt} = v \tag{6}$$

and

$$\frac{dX}{dt} = u_V \tag{7}$$

$$\frac{dY}{dt} = v_V \tag{8}$$

The numerical method employed is similar to that of Pullin[1] (see also Ref. 17), except that we consider a nonperiodic domain with a point vortex. An analytic solution for the influence of the unperturbed interface is used, leaving only the influence of the displacement of the interface to be calculated numerically. This allows us to limit the computational domain to a region near the vortex (where the interface is significantly displaced), yielding a substantial computational savings.[9] The spatial integration of Eqs. (2) and (3) was carried out using the trapezoidal rule, and the time integration was done using a second-order Adams–Bashforth predictor–corrector scheme. Note that the expression for the velocity, Eq. (2), is particularly suitable for accurate numerical quadrature because it no longer involves a singular kernel.

The numerical method was verified by extensive comparisons with the linear theory in Ref. 9. Here, where highly nonlinear results are being simulated, departures from conservation of circulation and the x component of momentum are used as measures of the accuracy of the code. Conservation of circulation implies that the area swept out by the disturbance does not change with time:

$$\frac{d}{dt}\left\{\int_{-\infty}^{\infty}[H(x, t) + \tilde{\Gamma}]\, dx\right\} = 0 \tag{9}$$

As discussed by Bell,[7,8] momentum transfer between the vortex and the layer results conserves the x component of momentum:

$$Y(t) - Y(0) = -(1/2\tilde{\Gamma})\left[\|H\|^2 - \|H_0\|^2\right] \tag{10}$$

revealing that the change in vertical position of the vortex is proportional to the norm of the disturbance to the interface, $\|H\|^2$, where

$$\|H\|^2 = \int_{-\infty}^{\infty}[H(x, t)]^2\, dx \tag{11}$$

Spatial and temporal refinement were used to verify conservation of circulation and x momentum. In practice, the relative error in x momentum was at most 10^{-4}. The most sensitive measure of accuracy was conservation of circulation. The integrations were terminated when the error was greater than 0.005, corresponding to 0.5% of the circulation in a unit length of the layer.

IV. Scaling

The vortex strength and initial height are chosen such that $\tilde{\Gamma}/[Y(0) - 1]$ is constant. The initial perturbation is due solely to the presence of the vortex and its image as described by the third and fourth terms on the right-hand side of Eq. (2). With $\tilde{\Gamma}/[Y(0) - 1]$ constant, the initial vortex-induced velocity along the interface will

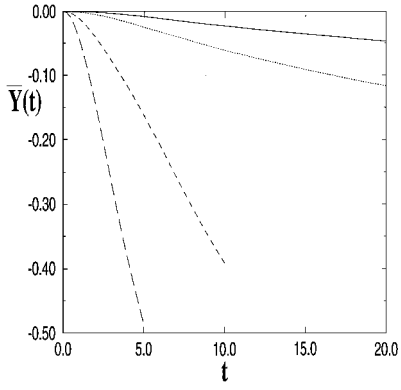

Fig. 2 Variable $\bar{Y}(t) = [Y(t) - Y(0)]/[Y(0) - 1]$ gives the displacement of the vortex relative to its initial height above the interface. In case 1 (——) and case 2 (· · · · ·), the change in the height of the vortex is not significant. In case 3 (- - - -) and case 4 (– – –), the time variation of the vortex height must be accounted for to accurately predict boundary-layer deformation.

appear identical in all cases when considered as a function of the scaled variable

$$\bar{x} \equiv x/[Y(0) - 1] \tag{12}$$

The effects of the image vortex cannot be so neatly scaled, but for cases in which the vortex is far above the wall {and keeping $\tilde{\Gamma}/[Y(0) - 1]$ constant} the initial image-induced velocity also is a function of $\bar{x}$ alone, to leading order. For heights that place the vortex close to the interface, $[Y(0) - 1]$ small, the initial image-induced velocity will vary from case to case, but over the range studied this variation is at most about 39% for v and about 29% for u. The dominant variation from case to case is that the initial deformation of the boundary layer will be spread over a wider interval when the vortex is farther above the wall than when it lies closer. The subsequent self-interaction of the deformed boundary layer is affected by this length scale.

Not only does the point vortex induce deformations in the boundary layer, but also the deforming boundary layer will induce a velocity on the point vortex. This can be seen from Eq. (3). The first two terms on the right-hand side show that deformations to the vortex layer influence both the horizontal and vertical position of the point vortex. When the point vortex is far above the boundary layer $[Y(0) \gg 1]$, the velocity field induced by the perturbed interface on the vortex will be smaller than when a weaker vortex {but $\tilde{\Gamma}/[Y(0) - 1]$ held constant} is placed close to the interface. Note that the deformation of the boundary layer is coupled to the motion of the vortex: the point vortex deforms the boundary layer, which itself affects the position of the point vortex, and so modifies the vortex's subsequent effects on the boundary layer, and so on.

The absolute vertical displacement of the vortex, $Y(t) - Y(0)$, indicates the extent of momentum transfer between the point vortex and the layer; see Eq. (10). The relative change of velocity at the interface due to vertical motion of the vortex can be gauged by the relative vertical displacement $\bar{Y}(t) \equiv [Y(t) - Y(0)]/[Y(0) - 1]$; see Fig. 2.

V. Results

In this section, we consider four cases of a strong vortex ($\tilde{\Gamma} \gg 1$) placed above the interface $[Y(0) > 1]$ where the lateral position of the vortex is initially set at $X(0) = 0$. The values of the parameters for the four cases are shown in Table 1. The parameter $\tilde{\Gamma}/[Y(0) - 1]$, which controls the vortex-induced velocity, is kept constant, whereas the strength of the vortex $\tilde{\Gamma}$ and its initial height $Y(0)$ are varied.

For case 1, Fig. 3 shows the evolution of the interface in the presence of a point vortex that is placed far above the interface $[Y(0) = 9]$ with strength $\tilde{\Gamma} = 64.0$ and with the interface initially located at $y = 1$. The vortex lies above the interface outside of the view shown: The small open triangle marks the x position of the vortex; its y position is off the scale. For very short times, not shown, an antisymmetric disturbance forms, consisting of a hump downstream of the point vortex and a trough upstream of the vortex. As time progresses, the growing hump propagates downstream faster than the vortex, and a broadening depression of the interface is seen at $t = 5$. By $t = 10$ the rate of growth of the disturbance slows, although it has significantly steepened on its upstream side. Also, incipient entrainment of irrotational flow toward the wall and in the downstream direction is observed. At $t = 20$, the interface has overturned, and the irrotational flow has penetrated into the vortex layer in the form of a thin crevice that grows in the downstream direction. As the vortex becomes increasingly distant from the disturbance, its influence wanes. However, the rate of entrainment increases as the irrotational flow approaches the wall. This implies that the wall, i.e., the image vorticity, plays a dominant role in entrainment.

Table 1 Parameter values for the four cases

Parameter	Case 1	Case 2	Case 3	Case 4
$Y(0)$	9	6	3	2
$\tilde{\Gamma}$	64	40	16	8
$\tilde{\Gamma}/[Y(0) - 1]$	8	8	8	8

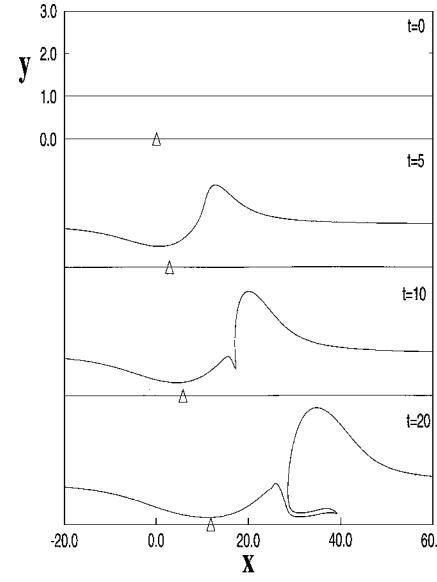

Fig. 3 Case 1: the evolution of the interface subject to a vortex of strength $\tilde{\Gamma} = 64$ initially at $Y(0) = 9$. Four times $0 \le t \le 20$ are shown. The vortex lies outside of the view shown; its x location is indicated by an open triangle.

Figure 2 shows the relative height of the point vortex $\bar{Y}(t)$ as a function of time. The variable $\bar{Y}(t)$ provides a measure of the degree to which the vortex displacement modifies the evolution of the layer. As seen in Fig. 2, the vertical displacement of the vortex in case 1 is small relative to its initial height above the interface. Moreover, the rate at which the vortex descends toward the interface appears to diminish slowly with time.

In case 2, as shown in Fig. 4, the vortex is closer to the interface (but still far above it), $Y(0) = 6$, and weaker, $\tilde{\Gamma} = 40$. The vortex is off the scale, but its x location is indicated by the small open triangle. The early-time behavior exhibits rapid growth that by $t = 5$ appears to slow. The disturbance continues to steepen, however, and by $t = 10$ begins to overturn. As it overturns, irrotational flow is entrained in a deepening wedge, $t = 20$. The shape of the interface takes a form similar to that of case 1; however, the timescale with which this occurs is faster in this case. Furthermore, the length scale is shorter, as suggested by the scaling based on $\bar{x}$, Eq. (12).

In Fig. 2 we see that for this case the magnitude of the vortex displacement, $\bar{Y}(t)$, toward the interface is nearly twice that of the preceding case, indicating that the interaction is stronger. However, the descent of the vortex still occurs on a timescale that is very slow compared with the timescale upon which the interface evolves.

In case 3, the vortex is placed at $Y(0) = 3$ with strength $\tilde{\Gamma} = 16$. Figure 5 shows the evolution of the interface deformation, and the accompanying location of the vortex is shown as the small circle. In

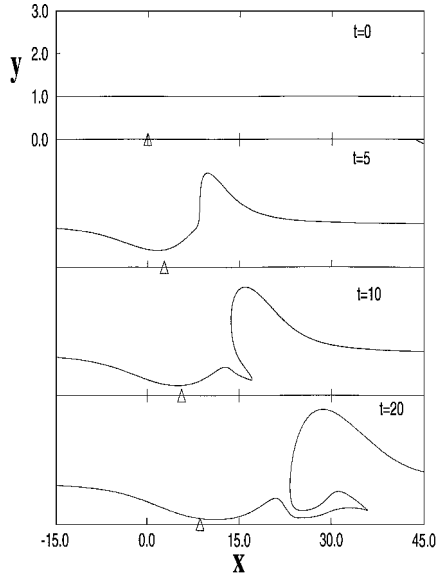

Fig. 4 Case 2: the evolution of the interface subject to a vortex of strength $\tilde{\Gamma} = 40$ initially at $Y(0) = 6$. Four times $0 \le t \le 20$ are shown. The vortex is outside of the view shown; its x location is indicated by an open triangle.

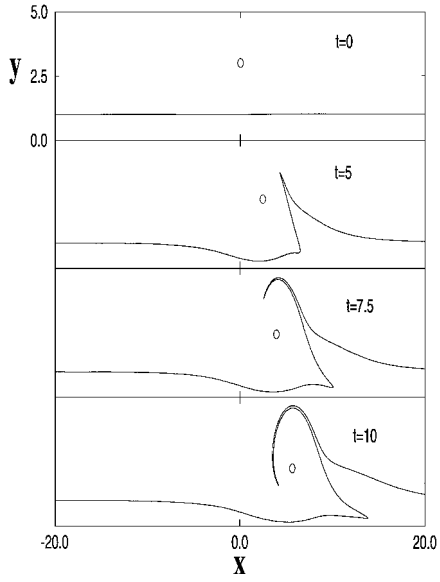

Fig. 5 Case 3: the evolution of the interface subject to a vortex of strength $\tilde{\Gamma} = 16$ initially at $Y(0) = 3$. Four times $0 \le t \le 10$ are shown. The location of the vortex is indicated by the small circle.

this case, all four snapshots of the interface evolution indicate rapid growth and steepening. Moreover, instead of the growth saturating, the disturbance focuses into a narrowing spike of erupting vorticity. Note that the apex of the erupting filament goes well beyond the vertical height of the vortex. Finally, after $t = 5$ the erupting filament begins to roll up and around the descending point vortex. The growth of the amplitude of the disturbance occurs on a much faster timescale than in the preceding two cases.

Figure 2 shows the relative height $\bar{Y}(t)$ of the vortex in case 3 as a function of time. The rate of descent of the vortex toward the interface is increasing with time. By $t = 5$ the displacement of the vortex is a significant fraction of the initial height of the vortex. Although in the preceding two cases the boundary-layer deformation for all times shown could have been well approximated by using the induced velocity of a point vortex fixed at its initial height, here the downward displacement of the vortex cannot be neglected. To accurately compute the induced velocity at the interface, the vertical displacement of the vortex must be accounted for.

In case 4, as shown in Fig. 6, the vortex is placed at $Y(0) = 2$ with strength $\tilde{\Gamma} = 8$. The position of the point vortex is shown by a

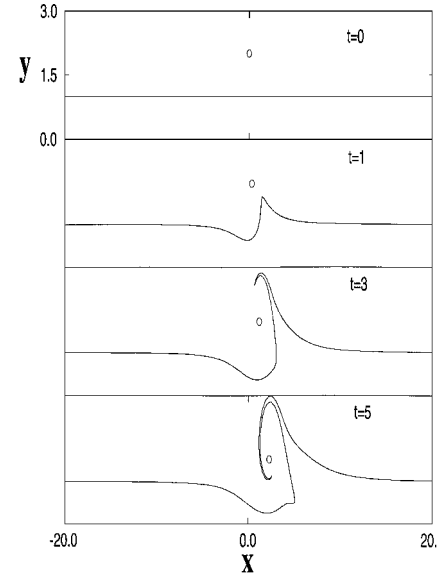

Fig. 6 Case 4: the evolution of the interface subject to a vortex of strength $\tilde{\Gamma} = 16$ initially at $Y(0) = 2$. Four times $0 \le t \le 5$ are shown. The location of the vortex is indicated by the small circle.

small circle. In this case, an erupting, narrowing plume of vorticity is ejected into the irrotational flow on a very fast timescale. As the filament continues to grow and steepen, the contour becomes multivalued and is followed by the roll up of the filament around the vortex. Recall that in the preceding case the eruptive filament reached a larger amplitude by $t = 5$ but had not reached the roll-up stage. Figure 2 details the changes in relative height of the vortex. The downward displacement of the vortex is a significant fraction of the initial height in this case.

VI. Discussion

Four cases in which the vortex induces a large velocity on the boundary layer have been examined. In each case, the initial height of the vortex above the layer was prescribed while the ratio of the vortex circulation to the height of the vortex above the interface was kept fixed. As was seen in Sec. V, changing the initial height of the vortex yields two significant changes in the interaction between the vortex and interface. First, the horizontal extent of the boundary-layer deformation scales with vortex height, i.e., the farther the vortex is placed above the layer, the longer the length scale of its induced perturbation. This length scale affects the boundary-layer self-interaction. Second, the velocity induced by the layer on the vortex varies as a function of the height of the vortex.

In cases 1 and 2, the vortex is far above the interface, resulting in a long-wavelength disturbance. A narrow wedge of irrotational flow penetrates the layer and is entrained downstream once it gets sufficiently close to the wall. The growth of the broad mound of vorticity seen in Figs. 3 and 4 appears to slow, and its amplitude appears to saturate. This large vortical disturbance also propagates downstream with a speed that is greater than that of the vortex (as is indicated by the increasing distance between the disturbance and the horizontal location of the vortex). Hence we surmise that the effect of the boundary layer on the vertical displacement of the vortex may diminish for very long times. This process was shown to occur for the case of small-amplitude waves in Ref. 9. There it was demonstrated that the motion of the vortex reached a steady state for long times because the interfacial waves propagated downstream faster than the vortex.

The path lines of the vortex for cases 1 and 2 indicate that the vortex moves only a small fraction of the initial vortex height; see Fig. 2. As a result, for the timescales considered, the change in the position of the vortex has only a minor effect on the velocity induced on the interface. Furthermore, the rate of descent of the vortex appears to diminish with time as the distance between the horizontal location of the vortex and the vortical disturbance increases.

In cases 3 and 4, the vortex is initially placed closer to the boundary layer: consequently, shorter length-scale disturbances result.

Due in part to the slenderness of the disturbance seen in Figs. 5 and 6, the erupting fluid, although large in vertical extent, induces only a small velocity field. Moreover, in contrast to the deformations seen here, unforced vortex layers do not exhibit rapid growth[1,17] and are known to be linearly stable.[18] Hence it appears that the eruption and continual narrowing of the filament is dominated by the presence of the point vortex.

The erupting layer induces a velocity on the vortex that draws it toward the interface. As is shown in Fig. 2, the descent of the vortex cannot be neglected in cases 3 and 4. In addition, the disturbance propagates away from the vortex at a slower rate than in cases 1 and 2. Thus, the mutual interaction between the vortex and the layer appears to be a necessary ingredient in determining the evolution of the interface.

VII. Conclusions

In summary, the model indicates that a vortex far from the boundary layer yields long-wavelength disturbances that evolve on slow timescales. These disturbances are large and broad enough to induce a velocity on themselves that is of the same order as the vortex. Also, the speed of long disturbances is fast, leading to a rapid loss of interaction between the vortex and the disturbance. As a result, the vortex-induced growth saturates. Entrainment of irrotational flow dominates the long-time dynamics as a crevice gets stretched by the wall. The form of the disturbance suggests a vortex-like structure and implies that a strong vortex located far above the boundary layer may act to generate another vortex-like disturbance within the boundary layer.

A vortex close to a boundary layer generates short-scale disturbances that erupt into the irrotational flow on a fast timescale and roll up. The descent of the vortex toward the interface may act to enhance the growth. Furthermore, as short-scale disturbances propagate slowly, the continued correlation of the x location of the vortex and the disturbance tends to focus the disturbance into an eruptive filament that accumulates energy at the expense of the vortex.

The approach presented here can be expected to be applicable to flows at high Reynolds numbers. In this regime, these results extend the calculation of the dynamics to the interactive stage, thereby making possible the study of interface evolution through the stages of overturning and roll up.

Acknowledgments

The authors appreciate the support of the National Science Foundation under Grant CTS-9206828. The first author would also like to thank the Department of Mechanical Engineering at Northwestern University for his support under the Pentair Teaching Fellowship.

References

[1] Pullin, D. I., "The Nonlinear Behaviour of a Constant Vorticity Layer at a Wall," *Journal of Fluid Mechanics*, Vol. 108, 1981, pp. 401–421.

[2] Dritschel, D. G., "The Repeated Filamentation of Two-Dimensional Vorticity Interfaces," *Journal of Fluid Mechanics*, Vol. 194, 1988, pp. 511–547.

[3] Pullin, D. I., Jacobs, P. A., Grimshaw, R. H. J., and Saffman, P. G., "Instability and Filamentation of Finite-Amplitude Waves on Vortex Layers of Finite Thickness," *Journal of Fluid Mechanics*, Vol. 209, 1989, pp. 359–384.

[4] Pullin, D. I., "Contour Dynamics Methods," *Annual Review of Fluid Mechanics*, Vol. 24, 1992, pp. 89–135.

[5] Jiménez, J., and Orlandi, P., "The Rollup of a Vortex Layer," *Journal of Fluid Mechanics*, Vol. 248, 1993, pp. 297–313.

[6] Stern, M. E., and Flierl, G. R., "On the Interaction of a Vortex with a Shear Flow," *Journal of Geophysical Research*, Vol. 92, 1987, pp. 10,733–10,744.

[7] Bell, G. I., "Interaction Between Vortices and Waves in a Simple Model of Geophysical Flow," *Physics of Fluids*, Vol. 2, No. 4, 1990, pp. 575–586.

[8] Bell, G. I., "Vortex-Induced Radiation Transported by a Contour," *Physica D*, Vol. 44, 1990, pp. 203–228.

[9] Atassi, O. V., Bernoff, A. J., and Lichter, S., "The Interaction of a Point Vortex with a Wall-Bounded Vortex Layer," *Journal of Fluid Mechanics*, Vol. 343, 1997, pp. 169–195.

[10] Walker, J. D. A., "The Boundary Layer due to Rectilinear Vortex," *Proceedings of the Royal Society of London, Series A*, Vol. 359, 1978, pp. 167–188.

[11] Van Dommelen, L. L., and Shen, S. F., "The Spontaneous Generation of the Singularity in a Separating Laminar Boundary Layer," *Journal of Computational Physics*, Vol. 38, 1980, pp. 125–140.

[12] Peridier, V. J., Smith, F. T., and Walker, J. D. A., "Vortex-Induced Boundary Layer Separation. Pt. 1: The Unsteady Limit Problem $Re \to \infty$," *Journal of Fluid Mechanics*, Vol. 232, 1991, pp. 99–131.

[13] Peridier, V. J., Smith, F. T., and Walker, J. D. A., "Vortex-Induced Boundary Layer Separation. Pt. 2: Unsteady Interacting Boundary Layer Theory," *Journal of Fluid Mechanics*, Vol. 232, 1991, pp. 99–131.

[14] Doligalski, T. L., Smith, C. R., and Walker, J. D. A., "Vortex Interactions with Walls," *Annual Review of Fluid Mechanics*, Vol. 26, 1994, pp. 573–616.

[15] Bernoff, A. J., van Dongen, H. J. H. M., and Lichter, S., "The Steady Boundary Layer due to a Fast Vortex," *Physics of Fluids*, Vol. 8, No. 1, 1996, pp. 156–162.

[16] Milne-Thomson, L. M., *Theoretical Hydrodynamics*, Macmillan, London, 1968, pp. 50–53.

[17] Stern, M. E., and Pratt, L. J., "Dynamics of Vorticity Fronts," *Journal of Fluid Mechanics*, Vol. 161, 1985, pp. 513–532.

[18] Lord Rayleigh (J. W. Strutt), "On the Stability or Instability of Certain Fluid Motions, II," *Scientific Papers*, Vol. 3, Cambridge Univ. Press, Cambridge, England, UK, 1902, pp. 17–23.

G. M. Faeth
Editor-in-Chief